arXiv:1406.7058v1 [physics.atm-clus] 27 Jun 2014

From the "Brazuca" ball to Octahedral Fullerenes: Their Construction and Classification

Yuan-Jia Fan and Bih-Yaw Jin*

Department of Chemistry and Center for Emerging Material and Advanced Devices, National Taiwan University, Taipei 10617, Taiwan

(Dated: June 30, 2014)

Abstract

A simple cut-and-patch method is presented for the construction and classification for fullerenes belonging to the octahedral point groups, O or O_h. In order to satisfy the symmetry requirement of the octahedral group, suitable numbers of four- and eight-member rings, in addition to the hexagons and pentagons, have to be introduced. An index consisting of four integers is introduced to specify an octahedral fullerenes. However, to specify an octahedral fullerene uniquely, we also found certain symmetry rules for these indices. Based on the transformation properties under the symmetry operations that an octahedral fullerene belongs to, we can identify four structural types of octahedral fullerenes.

*Electronic address: byjin@ntu.edu.tw

I. INTRODUCTION

The 2014 FIFA World Cup championship in Brazil expected to attract the attention of more than 3 billion people worldwide is the quadrennial soccer tournament since 1930. Whereas, the most popular design for the FIFA soccer ball, the Telstar, which was used in the official logo for the 1970 World Cup, consists of twelve black pentagonal and 20 white hexagonal panels, a truncated icosahedron belonging icosahedral point group[1, 2]. Since then, a number of different designs have appeared, some with small variations such as the Fevernova (2002) and the Teamgeist (2006) which still have icosahedral symmetry but with low-symmetry tetrahedral patterns painted on the ball; some balls only show lower polyhedral patterns such as Jabulani (2012) with tetrahedral symmetry without icosahedral symmetry superimposed. However, the soccer ball, "Brazuca" ball, used for the World Cup this summer in Brazil has a new design based on octahedral symmetry. Basically, the "Brazuca" ball is composed of six bonded polyerethane panels with four-arm clover-shaped panels that interlock like a jigsaw puzzle smoothly on a sphere[3, 4].

In 1985, it was discovered that, in addition to diamond and graphite, carbon atoms can have a third new allotrope consisting of 60-atom spherical molecules, C_{60}, sometimes nicknamed molecular soccer ball because the shape of this molecule is identical to the standard soccer ball, with 60 atoms located at 60 identical vertices[5]. More generally, this molecule belongs to a family of sp^2-hybridized pure carbon systems now called fullerenes that contain only five- and six-membered rings. Since then, structures of fullerenes have been extensively studied experimentally and theoretically. Under this constraint, considerable effort has been devoted to detailed enumerations of possible structures. For instance, a complete list of fullerenes with less than or equal to 60 carbon atoms and all fullerenes less than and equal to 100 carbon atoms that satisfy the isolated pentagon rule (IPR) is tabulated in the monograph by Fowler and Manolopolous[6]. Among all these fullerenes C_N, $N \leq 100$, the possible symmetry point groups for fullerenes are C_1, C_s, C_i, C_m, C_{mv}, C_{mh}, S_{2m}, D_n, D_{nd}, D_{nh}, T, T_d, T_h, I and I_h, where m can be 2 or 3 and n can be 2, 3, 5 or 6. However, only two out of three Platonic polyhedral groups, namely tetrahedral and icosahedral groups, seems to be possible for fullerenes. So the question is, can we have fullerenes with octahedral symmetry just like the "Brazuca" ball? If possible, what are the general construction and classification rules for this family of octahedral fullerenes?

To answer this question, we start with the construction process of fullerenes with polyhedral symmetries through a simple cut-and-patch procedure as shown in Figure 1. For instance, constructing a fullerene with icosahedral symmetry can be done by cutting 20 equivalent equilateral triangles from graphene and pasting them onto the triangular faces of an icosahedron. This will create twelve pentagons sitting at twelve vertices of the icosahedron[7–9]. Similar cut-and-patch procedure can be used to construct fullerenes with tetrahedral and octahedral symmetries, too (Figure 1). However, the non-hexagons such as triangles and squares will appear at the vertices of the template tetrahedron and octahedron, which are in contradiction to the definition of fullerenes. In the case of tetrahedral fullerenes, we can replace the template tetrahedron with a truncated tetrahedron. This makes it possible to the construction of tetrahedral fullerenes without triangles by a suitable cut-and-patch construction scheme[10]. But this technique is not applicable to octahedral fullerenes[11, 12].

Albeit the appearance of squares in these caged octahedral fullerenes leads to energetically unstable molecules, one can still find in literatures that some studies have been carried out on the geometric, topological[13], and electronic structures[14–17] of fullerenes with octahedral symmetry by introducing squares on a template octahedron (Figure 1). In addition to the pure carbon allotropes, the octahedral boron-nitride systems have also been vigorously investigated[18–22].

In this paper, we present a general cut-and-patch construction and classification scheme for fullerenes with octahedral symmetry by systematically introducing some other non-hexagons such as octagons with a cantellated cube as the template. The octahedral fullerenes previously considered in literatures are included as limiting cases in our general construction scheme[13–17]. We also like to point out that the cut-and-patch method is a simple and powerful method for building various kinds of fullerenes and graphitic structures. For instance, we have applied this method successfully to many other template polyhedral tori and concluded general structural rules of carbon nanotori[23, 24]. From there, structural relations for a whole family of topologically nontrivial fullerenes and graphitic structures such as carbon nanohelices, high-genus fullerenes, carbon Schwarzites and so on can be derived[25–28].

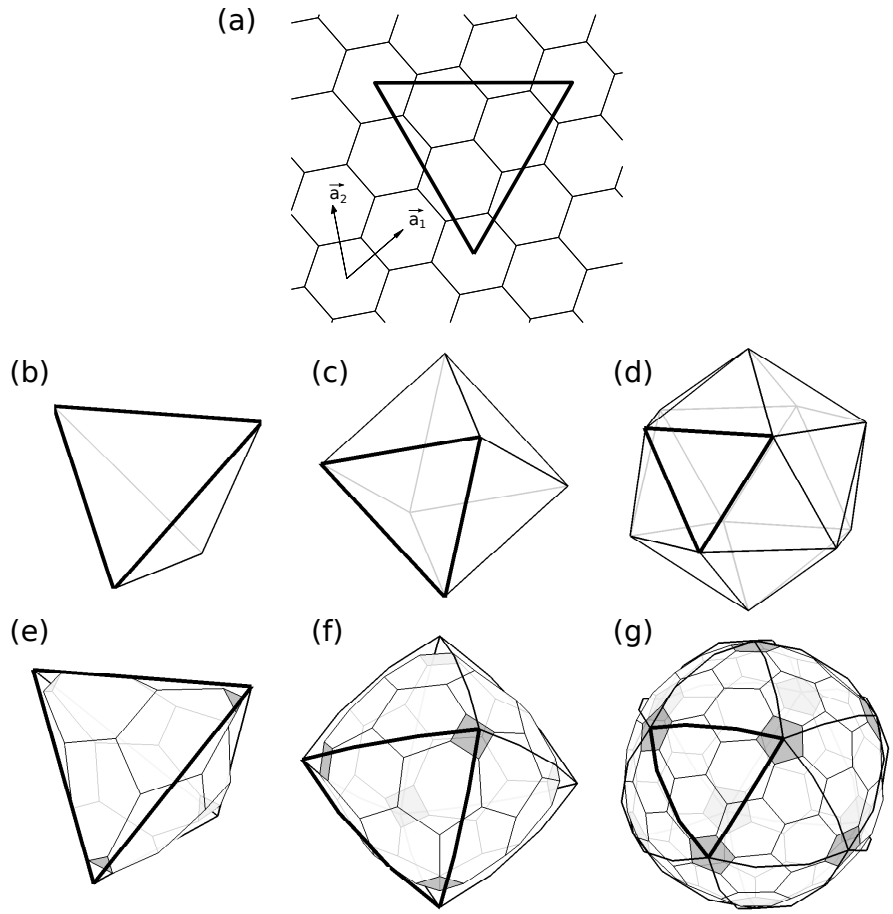

FIG. 1: Goldberg polyhedra by the cut-and-patch construction. Here we cut a equilateral triangle which can be specified by an vector $(2, 1)$ (also known as Goldberg vector) from graphene and then patch the triangle onto different platonic solids to construct fullerenes with different polyhedral symmetries. The famous C_{60}, can be also constructed in this way using icosahedron as the template with Goldberg vector (1,1).

II. REQUIREMENT OF OCTAHEDRAL FULLERENES

We start by briefly describing the icosahedral fullerenes that consist only of hexagons and pentagons. The simplest icosahedral fullerene that satisfies IPR is C_{60}, which can also be viewed as a truncated icosahedron, one of the thirteen Archimedean solids if we ignore the slight variation in bond lengths. In a truncated icosahedron, there are exactly twelve pentagons and twenty hexagons. This structure can be derived from a regular icosahedron by truncating the twelve vertices away appropriately. We will show that this is the only

possibility if we want to construct an icosahedral fullerene with pentagons and hexagons only.

Using the Euler's polyhedron formula, $V - E + F = 2$ for a polyhedron with V vertices, E edges and F faces, and the condition $3V = 2E$ for trivalent carbon atoms in a fullerene, we can find easily the condition $\sum_n (6-n)F_n = 12$, where F_n is the number of n-gons. If we assign each face a topological charge $6 - n$, the Euler's polyhedron formula states that the sum of topological charges of a trivalent polyhedron must be twelve. Therefore, fullerenes that contain only pentagons and hexagons must have twelve pentagons, i.e. $F_5 = 12$, while there is no constraint on the number of hexagons, F_6, except the case with only one hexagon, $F_6 = 1$, is forbidden. This conclusion is general and can be applied to any fullerene regardless of its symmetry.

An arbitrary icosahedral fullerene can be classified by its chiral vector (h, k), where h and k satisfy the inequality $h \geq k \geq 0 \wedge h > 0$, according to the Goldberg construction [7]. For instance, C_{60} corresponds to the fullerene with chiral vector $(1, 1)$. Interestingly, these twelve pentagons are located at the high-symmetry points along the six fivefold rotational axes of the icosahedral symmetry group. Suppose that these pentagons are not located at the high symmetry points, there should be five pentagons around each of these points in order to satisfy the symmetry requirement. Therefore, there must be $12 \times 5 = 60$ pentagons in total. However, the condition, $\sum_n (6 - n)F_n = 12$, will require some n-gons where $n > 6$ to compensate the extra topological charges introduced by these pentagons. So, we conclude that exactly twelve pentagons must be located at the high symmetry points along the six fivefold rotation axes.

We apply the above analysis to the requirement for octahedral fullerenes. First, there are three fourfold axes, four threefold axes, and six twofold axes in the octahedral group. Pentagons are not compatible with any of the high symmetry points of octahedral groups. Therefore, there is no high symmetry point where pentagons can be located. The best we can do is to put clusters of pentagons around, for example, the three fourfold axes. Then we need to put twenty-four pentagons together with n-gons where $n > 6$ to balance the topological charges. A simple way is to put six octagons at the six high symmetry points along three fourfold axes, so that the condition, $\sum_n (6-n)F_n = 12$, is satisfied. The twofold or the fourfold axes can also be chosen[11], but the resulting fullerenes are considerably more energetically unfavored because additional non-hexagons need to be introduced.

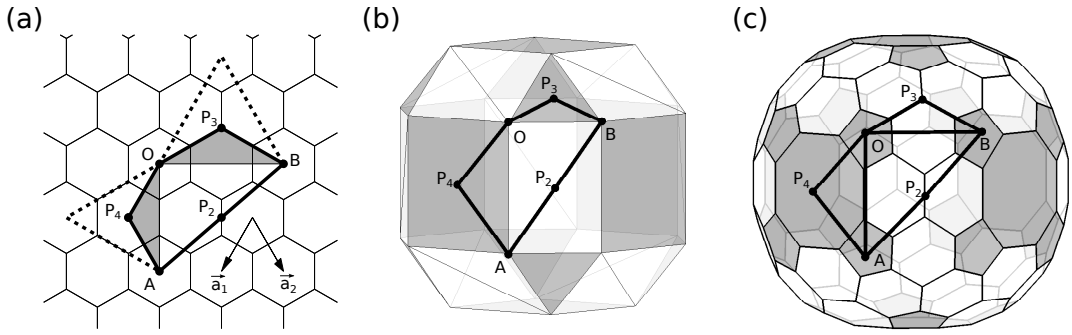

FIG. 2: Cut-and-patch procedure for constructing an octahedral fullerene. Points, P_2, P_3 and P_4, represent the high symmetry points of the octahedral symmetry respectively. $\triangle OP_4A$ ($\triangle OP_3B$) is one-third of a regular triangle (the dotted triangle in (a)) and P_4 (P_3) is the corresponding triangle center on graphene. Points O, A, and B become positions where twenty-four equivalent pentagons are located at, while point P_4 becomes the position for one of six equivalent octagons after they are patched onto the cantellated cube. The two base vectors, $\overrightarrow{OA} = (i, j)$ and $\overrightarrow{OB} = (k, l)$, can in general be any two vectors such that P_4 does not coincide with an atom (*i.e.*, $i - j = 3n$). $\{i, j, k, l\} = \{1, 1, -2, 2\}$ in this example. (c) The 3D geometry of an octahedral fullerene specified according to its topological coordinates [9].

To illustrate this idea, we present a simple construction procedure using the cut-and-patch scheme as shown in Figure 2. We first cut the polygonal region as defined by the solid thick line from graphene (Figure 2(a)) and then patch twenty-four replica of it on a cantellated cube as shown in Figure 2(b). The points, O, A, and B in Figure 2(a) overlap with vertices of the cantellated cube while P_3 and P_4 the centers of the triangle and the square faces, respectively. In this process, every four identical isosceles triangles, $\triangle OP_4A$, cover one square face (Figure 2(b)). Since the angular deficit at P_4 is $2\pi - 4 \times 2\pi/3 = -2\pi/3$, it must correspond to the location of an octagon. On the other hand, the angular deficit at O is $2\pi - (\pi + 2\pi/3) = \pi/3$. Therefore a pentagon will be generated at O by this cut-and-patch process.

We will define the area inside the solid thick line as shown in Figure 2(a) as the fundamental polygon. Note that the two base vectors, $\overrightarrow{OA} = (i, j)$ and $\overrightarrow{OB} = (k, l)$, in the fundamental polygon become the edges of the square and the regular triangle on the cantellated cube, respectively, as shown in Figure 2(b). For convenience, we refer to (i, j) as the

square base vector and (k, l) the triangular base vector from now on. Using these two vectors, we can uniquely specify a scalene triangle with four integers $\{i, j, k, l\}$, which we will simply call the indices of octahedral fullerenes later. In additional to this scalene triangle, we also need to incorporate two extra triangles, $\triangle OP_4A$ and $\triangle OP_3B$, corresponding to one-third of the regular triangles which share the same edges with the scalene triangle. The numbers of carbon atoms inside $\triangle OP_4A$, $\triangle OP_4A$, and $\triangle OAB$ are $(i^2+ij+j^2)/3$, $(k^2+kl+l^2)/3$, and $|il-jk|$, respectively. After patching twenty-four fundamental polygons onto a cantellated cube, we get an octahedral fullerene with $8(i^2+ij+j^2+k^2+kl+l^2)+24|il-jk|$ carbon atoms.

The octahedral fullerenes can be catagorized into two groups according to the sign of the angle θ formed by $\overrightarrow{OA}$ and $\overrightarrow{OB}$. Octahedral fullerenes with $\pi > \theta > 0$ are in category α, $\{i, j, k, l\}_\alpha$, and octahedral fullerenes $-\pi < \theta < 0$ are in category β, $\{i, j, k, l\}_\beta$. This criterion is equivalent to determining the sign of $il-jk$, which stands for the signed area enclosed by the parallelogram spanned by the two base vectors up to a positive factor. Here we can take one step further to include the degenerate cases, *i.e.* when $\triangle OAB$ degenerates into a line, which can be considered as limiting cases when θ approaches to the boundaries of its range in each category. It is worthwhile to note that in general $\lim_{\theta\to 0^+}\{i, j, k, l\}_\alpha$ is inequivalent to $\lim_{\theta\to 0^-}\{i, j, k, l\}_\beta$ and $\lim_{\theta\to \pi^-}\{i, j, k, l\}_\alpha$ is inequivalent to $\lim_{\theta\to \pi^+}\{i, j, k, l\}_\beta$, as shown in Figure 3. On the other hand, the category letter in the subscript can be omitted when there is no ambiguity. We will elaborate in later sections.

Following the above cut-and-patch scheme, we can define a scalene triangle and thus the fundamental polygon, given the two base vectors (i, j) and (k, l) that satisfy the condition, $i - j = 3n$. Each of these fundamental polygons uniquely defines an octahedral fullerene in non-degenerate case. When the two base vectors are parallel to each other, it is necessary to further specify the category explicitly. It is worthwhile to note that if the condition $i-j = 3n$ is not satisfied, P_4 will coincide with a carbon atom, which is not allowed because this implies that the carbon atom is tetravalent. At first sight, one might think that there exists a one-to-one correspondence between an index, $\{i, j, k, l\}_X$, and an octahedral fullerene. But this is not true since it is possible that the octahedral fullerenes built from two different scalene triangles are in fact identical. We will study this issue in details in the next section.

Finally we can identify three limiting situations if one of the three sides of the scalene triangle vanishes (see Fig. 4).

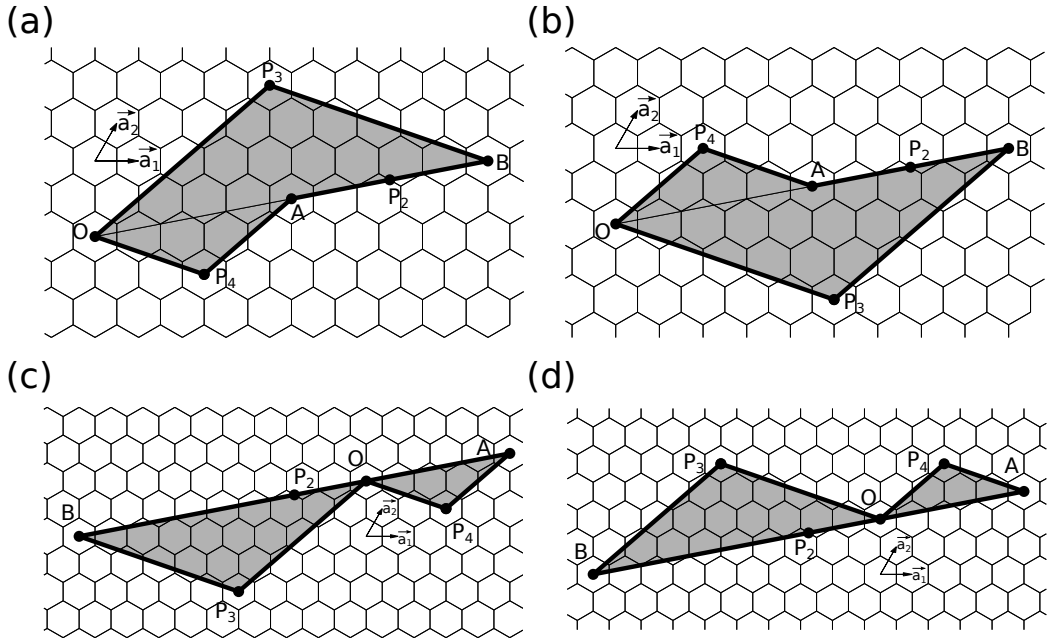

FIG. 3: Four degenerate cases of octahedral fullerenes. (a) $\{4,1,8,2\}_\alpha$, (b) $\{4,1,8,2\}_\beta$, (c) $\{4,1,-8,-2\}_\alpha$ and (d) $\{4,1,-8,-2\}_\beta$. We have $\{4,1,8,2\}_\alpha \neq \{4,1,8,2\}_\beta$ and $\{4,1,-8,-2\}_\alpha \neq \{4,1,-8,-2\}_\beta$. However, $T_2\{4,1,8,2\}_\alpha = \{4,1,-8,-2\}_\beta$ and $T_2\{4,1,8,2\}_\beta = \{4,1,-8,-2\}_\alpha$. The T_2 transformation will be discussed in later sections.

1. The first limiting situation corresponds to a vanishing triangular base vector, $(k,l) = (0,0)$, which is referred to as type I octahedral fullerenes later on. The indices for this case have the form $\{i,j,0,0\}$. Thus, the length of the triangular base vector $\overrightarrow{OB}$ vanishes and all triangles in the cantellated cube shrink to single points. And the template polyhedron reaches the corresponding limit of the cantellation, namely the cube. Note also that three pentagons fuse to form a triangle at each corner of the cube, while the octagons remain at the centers of the faces of the cube. Thus, there are eight triangles and six octagons in the resulting octahedral fullerene.

2. The second limiting situation corresponds to a vanishing square base vector, $(i,j) = (0,0)$, which we denote as type II. The indices for type II fullerenes are given by $\{0,0,k,l\}$. In this limit, the length of the square base vector $\overrightarrow{OB}$ vanishes and each square shrinks to a point. Thus, the template polyhedron reaches another limit of the cantellation, namely the octahedron. This case is identical to the Goldberg polyhedron

illustrated in Figure 1(c) and Figure 1(f) . Four pentagons and one octagon fuse to form a square at each corner of the octahedron. Therefore, we have six squares in a type II octahedral fullerene.

3. The last limiting situation, denoted as type III, is when the length of the third side of $\triangle OAB$, $\overrightarrow{AB}$, vanishes. In other words, $\overrightarrow{OA}$ is equal to $\overrightarrow{OB}$, i.e. $(i,j) = (k,l)$. One can show that $(i,j) = -(k,l)$ also corresponds to the same limiting case. $\{i,j,i,j\}$ and $\{i,j,-i,-j\}$ can be transformed to each other via additional symmetry transformations, T_3 or T_4, which will be introduced in the next section. The indices for this type are $\{i,j,i,j\}$ or $\{i,j,-i,-j\}$ and the template polyhedron in this limit is a cuboctahedron. Two pentagons at A and B fuse to become one square, and there are six octagons and twelve squares in total in this limiting case. Other collinear cases do not make the third side vanish though and pentagons will not fuse at all. In fact we can use T_3 or T_4 introduced later to make these two base vectors nonparallel.

When none of the sides of the scalene triangle vanishes, the corresponding octahedral fullerenes will be denoted as type IV.

III. INDEX SYMMETRY

In the previous section, we showed that an octahedral fullerene can be constructed by cutting a fundamental polygon specified by a four-component index and its category, $\{i,j,k,l\}_X$ and patching twenty-four replica of this fundamental polygon onto a cantellated cube. We also pointed that this correspondence is not one-to-one, but many-to-one, since there are some symmetry relationships in this indexing scheme. In other words, we mean that there exist different indices $\{i,j,k,l\}_X$ that correspond to the same molecular structure. This section is devoted to find a systematic way to eliminate all such redundancies and fully characterize the nature of the index symmetry.

In the limiting cases of octahedral fullerenes which belong to the types I to III, we only need one independent two-component vector to specify their indices. It is obvious that the index transformation arising from the geometric symmetry of graphene will lead to the same octahedral fullerene. For instance, a $\pi/3$ rotation about point O will transform the index from $\{i,j,k,l\}_X$ to $\{-j,i+j,-l,k+l\}_X$ without altering the resulting octahedral fullerene.

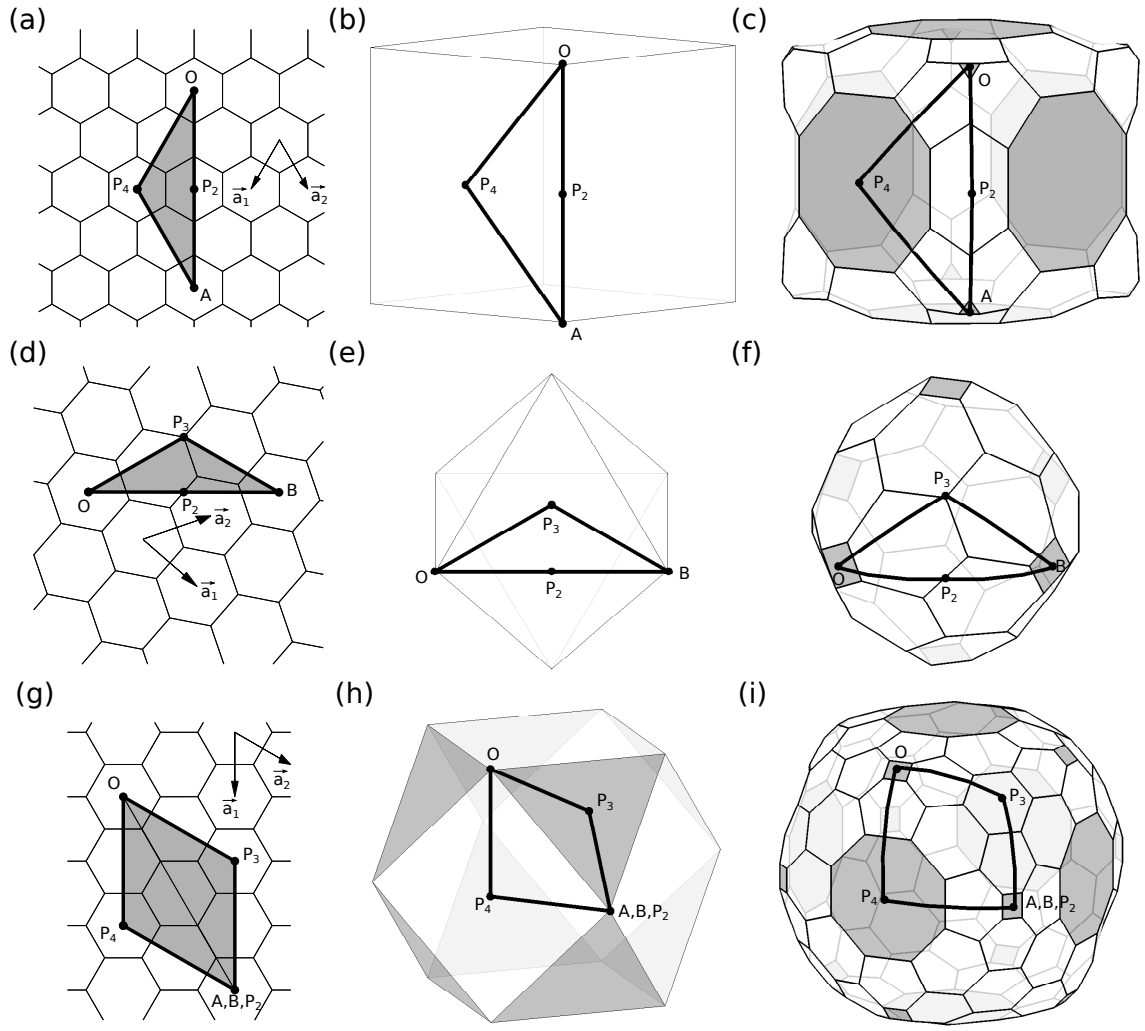

FIG. 4: Three limiting cases of octahedral fullerenes. (a)-(c) Type I octahedral fullerene with with $\{2,2,0,0\}$; (d)-(f) Type II octahedral fullerene with with $\{0,0,1,2\}$; (g)-(i) Type III octahedral fullerene with $\{2,2,2,2\}$. In this case points A, B, and P_2 are coincident.

Therefore these two indices correspond to the same molecular structure and should only be counted once. In fact, this applies to all twelve symmetry operations belonging to the point group C_{6v} of graphene. Here, we ignore symmetry operation σ_h that lies in the plane of graphene because it does not move any carbon atom at all. So, all indices that can be related through these symmetry operations produce the same octahedral fullerene. This set of indices is called an orbit in group theory[29]. So to enumerate octahedral fullerene is equivalent to enumerate different orbits of all possible indices. Indices belonging to the same orbit correspond to the same octahedral fullerene. In other words, only one out of the set of

indices comprising an orbit is needed to represent an octahedral fullerene uniquely. In these three limiting situations, we can restrict the indices with the inequality, $i \geq j \geq 0 \wedge i > 0$ for type I, $k \geq l \geq 0 \wedge k > 0$ for type II, and $i \geq j \geq 0 \wedge i > 0$ ($k = i$ and $l = j$) for type III to remove all redundancies arising from the $C_{6\mathrm{v}}$ symmetry operations.

The situation for type IV octahedral fullerenes is more complicated. In addition to the twelve symmetry operations from the point group C_{6v}, there are three more symmetry operations, T_2, T_3, and T_4 arising from different ways of dissecting each of the three different kinds of faces of a cantellated cube into fundamental polygons. For each dissection scheme, different squares or regular triangles are drawn, and the square or triangular base vectors will change respectively. Detailed description of these three symmetry operations will be described later. These extra symmetry operations introduce redundancies which cannot be removed by introducing inequalities of indices like the situations of types I to III.

Although the redundancies produced by these three T-type symmetry operations cannot be removed by such index restrictions, the parts of redundancies originating from the sixfold rotational symmetry of graphene can be eliminated by introducing the canonical criterion, $i > 0 \wedge j \geq 0$. This is because that these rotational operations commute with the three T-type operations, *i.e.* $[C_6^n, T_y] = 0$, where $y = 2$, 3 or 4. Here, we do not impose the restriction, $i \geq j$, to remove the redundancies produced by the six mirror symmetries M_x. This will be discussed with the T_2 symmetry in the next section.

A. T_2 symmetry

The symmetry operation, T_2, comes from the two different ways to decompose a parallelogram as shown in Figure 5. The T_2 operation stands for performing a local C_2 operation which rotate one of base vectors by 180°. Thus the index $\{i, j, -k, -l\}$ will generate the same octahedral fullerene with $\{i, j, k, l\}$. We can define T_2 explicitly with the following matrix notation

$$T_2 : \begin{pmatrix} i \\ j \\ k \\ l \end{pmatrix}_X \rightarrow \begin{pmatrix} i' \\ j' \\ k' \\ l' \end{pmatrix}_{X'} = \begin{pmatrix} 1 & 0 & 0 & 0 \\ 0 & 1 & 0 & 0 \\ 0 & 0 & -1 & 0 \\ 0 & 0 & 0 & -1 \end{pmatrix} \begin{pmatrix} i \\ j \\ k \\ l \end{pmatrix}_X ,$$

where $X \neq X'$.

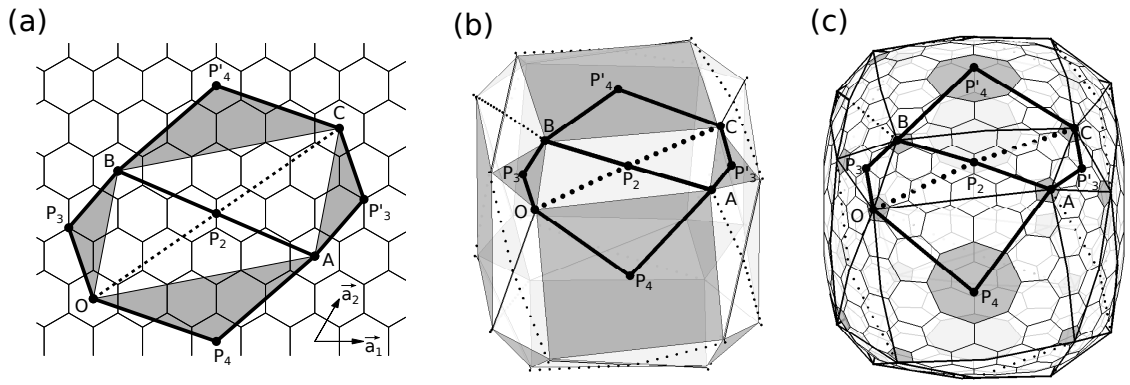

FIG. 5: The T_2 symmetry operation illustrated with the example $T_2\{4,1,-1,3\}_\alpha = \{4,1,1,-3\}_\beta$. If we choose $\{\overrightarrow{OA},\overrightarrow{OB}\}_\alpha$ as the index, the corresponding fundamental polygon is $OP_4AP_2BP_3$. On the other hand, if we choose the index $\{\overrightarrow{BC},\overrightarrow{BO}\}_\beta = \{\overrightarrow{OA},-\overrightarrow{OB}\}_\beta$, the fundamental polygon becomes $BP_4'CP_2OP_3'$. These two fundamental polygons essentially give the same octahedral fullerene with different ways of dissecting the parallelogram.

Unlike usual matrix multiplications, we need to specify the category of the index before and after T_2 transformation. Since $il - jk$ stands for the signed area enclosed by the parallelogram spanned by these two vectors up to a positive factor, it is clear that under the transformations, T_2 or M_x, the signed area changes sign and hence the category. This is also true in the degenerate case. Therefore, enumerating indices only in a single category can remove redundancies produced by T_2 and M_x, but not those produced by $M_xT_2 = T_2M_x$.

B. T_3 symmetry

The symmetry operation T_3 involves different ways of dissecting the equilateral triangles of the cantellated cube as shown in Figure 6. For instance, one possible choice of the two base vectors for the scalene triangle is $\{\overrightarrow{OA},\overrightarrow{OB}\}_\alpha$. However, there is another choice, $\{\overrightarrow{OA},\overrightarrow{OF}\}_\alpha$, which produce the same octahedral fullerene, but with a different way of dissecting the triangles of the cantellated cube. The T_3 transformation only changes the triangular base vectors.

Unlike T_2 and M_x, the T_3 transformation does not change the category. Moreover, for the $T_{3,\alpha}$ transformation, which operates on octahedral fullerenes belonging to the category α, we also need to impose an additional constraint on the domain $i'l' - j'k' \geq 0 \Rightarrow -ik - jk - jl \geq$

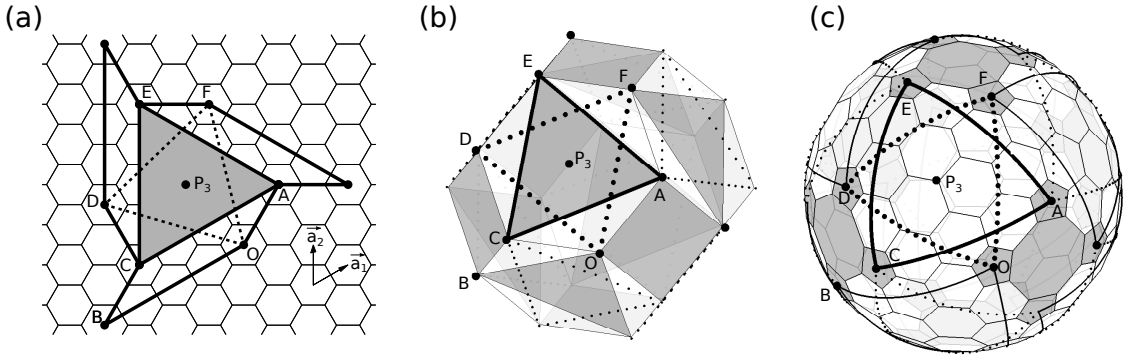

FIG. 6: An illustration of T_3 symmetry. T_3 transform the partition $\{\overrightarrow{OA}, \overrightarrow{OB}\}_\alpha = \{1, 1, -4, 0\}_\alpha$ to $\{\overrightarrow{OA}, \overrightarrow{OF}\}_\alpha = \{1, 1, -1, 4\}_\alpha$, which can be also written as $T_{3,\alpha}\{1, 1, -4, 0\}_\alpha = \{1, 1, -1, 4\}_\alpha$. Similarly we have $T_3^{-1}\{1, 1, -1, 4\}_\alpha = \{1, 1, -4, 0\}_\alpha$.

$i^2 + ij + j^2$. The explicit form of $T_{3,\alpha}$ can be written as

$$T_{3,\alpha} : \begin{pmatrix} i \\ j \\ k \\ l \end{pmatrix}_\alpha \rightarrow \begin{pmatrix} i' \\ j' \\ k' \\ l' \end{pmatrix}_\alpha = \begin{pmatrix} 1 & 0 & 0 & 0 \\ 0 & 1 & 0 & 0 \\ 2 & 1 & 1 & 1 \\ -1 & 1 & -1 & 0 \end{pmatrix} \begin{pmatrix} i \\ j \\ k \\ l \end{pmatrix}_\alpha .$$

We may obtain $T_{3,\beta}$ easily by $T_{3,\beta} = M_x T_{3,\alpha} M_x$ and its domain by similar method. The inverse of T_3 transformation, namely T_3^{-1}, may be found by the usual matrix inversion,

$$T_{3,\alpha}^{-1} : \begin{pmatrix} i \\ j \\ k \\ l \end{pmatrix}_\alpha \rightarrow \begin{pmatrix} i' \\ j' \\ k' \\ l' \end{pmatrix}_\alpha = \begin{pmatrix} 1 & 0 & 0 & 0 \\ 0 & 1 & 0 & 0 \\ -1 & 1 & 0 & -1 \\ -1 & -2 & 1 & 1 \end{pmatrix} \begin{pmatrix} i \\ j \\ k \\ l \end{pmatrix}_\alpha$$

Its domain can also be found by requiring that the category remains unchanged, $i'l' - j'k' \geq 0 \Rightarrow ik + il + jk \geq i^2 + ij + j^2$ and so we have the identity, $T_{3,\beta}^{-1} = M_x T_{3,\alpha}^{-1} M_x$. In addition, as shown in Figure 6, the T_3 transformation always decrease $|\theta|$ by more than $\pi/3$; while T_3^{-1} always increase $|\theta|$ by more than $\pi/3$.

C. T_4 symmetry

Similar to the symmetry operations T_2 and T_3, the operation T_4 involves different ways of assigning fundamental polygons on the cantellated cube as shown in Figure 7. In this

case, we can see that two different fundamental polygons given by indices $\{\overrightarrow{OA}, \overrightarrow{OB}\}_\alpha$ and $\{\overrightarrow{OF}, \overrightarrow{OB}\}_\alpha$ are essentially equivalent in constructing an octahedral fullerene. The transformation T_4 does not change the category just like the transformation T_3. We can interchange $T_{4,\alpha}$ and $T_{4,\beta}$ by sandwiching them between the mirror transformation M_x. On the other hand, in contrast to the transformation T_3, T_4 changes the square base vector only. Therefore, both T_3 and T_4 will decrease $|\theta|$ by more than $\pi/3$. In other words, the square base vector will be rotated by more than $\pi/3$ and will not satisfy the canonical criterion $i > 0 \wedge j \geq 0$ any longer. However the whole index can be rotated back to satisfy the canonical criterion again whenever necessary.

The explicit form for the symmetry operation $T_{4,\alpha}$ can be written as

$$T_{4,\alpha} : \begin{pmatrix} i \\ j \\ k \\ l \end{pmatrix}_\alpha \rightarrow \begin{pmatrix} i' \\ j' \\ k' \\ l' \end{pmatrix}_\alpha = \begin{pmatrix} 0 & -1 & 1 & -1 \\ 1 & 1 & 1 & 2 \\ 0 & 0 & 1 & 0 \\ 0 & 0 & 0 & 1 \end{pmatrix} \begin{pmatrix} i \\ j \\ k \\ l \end{pmatrix}_\alpha .$$

Again, an constraint on domain $-ik - jk - jl \geq k^2 + kl + l^2$ is necessary to ensure that the category stays unchanged. The inverse $T_{4,\alpha}^{-1}$ can be defined as follows

$$T_{4,\alpha}^{-1} : \begin{pmatrix} i \\ j \\ k \\ l \end{pmatrix}_\alpha \rightarrow \begin{pmatrix} i' \\ j' \\ k' \\ l' \end{pmatrix}_\alpha = \begin{pmatrix} 1 & 1 & -2 & -1 \\ -1 & 0 & 1 & -1 \\ 0 & 0 & 1 & 0 \\ 0 & 0 & 0 & 1 \end{pmatrix} \begin{pmatrix} i \\ j \\ k \\ l \end{pmatrix}_\alpha ,$$

and the constraint on the domain is $ik + il + jl \geq k^2 + kl + l^2$. In summary, C_6^n, T_3, T_4 and their inverses do not change the categories, but M_x and T_2 do.

Although T-type symmetry operations are defined for type IV octahedral fullerenes, they can also be applied to three limiting cases. When T-type symmetry operations are applied to type I and type II octahedral fullerenes, they reduce to the geometric rotation C_6^n. And when they are applied to type III octahedral fullerenes, we have following identities,

$$\begin{aligned} T_2\{i,j,i,j\}_X &= \{i,j,-i,-j\}_{X'} \quad (X \neq X') \\ T_3^{-1}\{i,j,i,j\}_X &= \{i,j,-i,-j\}_X \\ C_6^3 T_4^{-1}\{i,j,i,j\}_X &= \{i,j,-i,-j\}_X. \end{aligned}$$

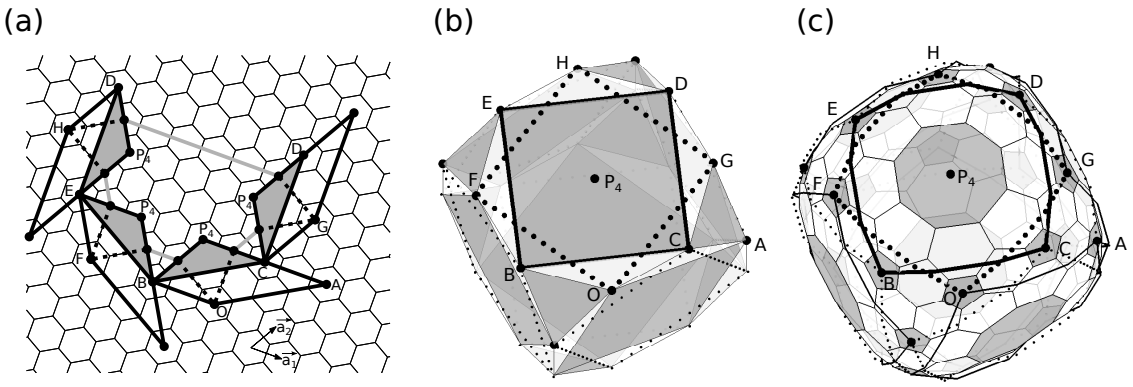

FIG. 7: An illustration of T_4 symmetry. T_4 transform the partition $\{\overrightarrow{OA}, \overrightarrow{OB}\}_\alpha = \{2, 2, -2, 0\}_\alpha$ to $\{\overrightarrow{OF}, \overrightarrow{OB}\}_\alpha = \{-4, 2, -2, 0\}_\alpha$, which can be also written as $T_{4,\alpha}\{2, 2, -2, 0\}_\alpha = \{-4, 2, -2, 0\}_\alpha$. Two points connected by a grey line should be patch into one point. Four shaded triangle in (a) will merge into square $BCDE$ in (b) and four P_4 points in (a) will become one P_4 in (b) after patching. Note that since P_4 always carries a topological charge, the vector $\overrightarrow{OF}$ does not correspond to $(-4, 2)$ in (a).

These formulae will give a torus-like orbit. The details for the enumeration of these orbits are included in supporting information.

IV. CONCLUSION

In conclusion, we have developed a systematic cut-and-patch method to generate arbitrary fullerenes belonging to the octahedral point group. A unique four-component vector satisfying certain constraints and symmetry rules can be used to specify these octahedral fullerenes. This work on the octahedral fullerenes fits in the final piece of the jigsaw puzzle of all possible high symmetry caged fullerenes based on Platonic solids. Further investigation on the stability, elastic properties and electronic structures of these octahedral fullerenes and the possibility of using them to build periodic carbon Schwarzites are currently undergoing in our group[28, 30].

Finally, we also want to point out two observations: the "Brazuca" ball used in the World Cup is close to a very round octahedral sphere, while the fullerenes discussed in this paper are still far from a round sphere. The explanation for the first observation is given in a more general context by Delp and Thurston in a paper about the connection between clothing

design and mathematics in the Bridges meeting three years ago.[31] The most important factor that makes it possible to wrap six clover-shaped panels used in the "Brazuca" around a sphere smoothly is that the curved seams created by these interlocked 4-long-arms panels are quite evenly distributed on the sphere. Readers interested in this problem should go to that paper for details. The observation on the shape of octahedral fullerenes is also interesting. All of the three-dimensional geometries shown in this paper are obtained through their topological coordinates derived from the lowest three eigenvectors with single nodes by diagonalizing the corresponding adjacency matrices[6]. Further investigations to rationalize how the distribution of the non-hexagons affects the shapes of octahedral fullerenes in order to obtain a round nanoscale "Brazuca" ball based on either elastic theory or quantum chemical calculations should be worth pursuing in the future.[6, 30, 32, 33]

acknowledgements

The research was supported by the Ministry of Science and Technology, Taiwan. B.-Y. Jin thanks Center for Quantum Science and Engineering, and Center of Theoretical Sciences of National Taiwan University for partial financial supports. We also wish to thank Chern Chuang and Prof. Yuan-Chung Cheng for useful discussions and comments on this paper.

---

[1] "Adidas Telstar." Wikipedia: The Free Encyclopedia. Wikimedia Foundation, Inc. (Accessed 17 Jul., 2014).

[2] Kotschick, D. The Topology and Combinatorics of Soccer Balls, *American Scientist* **2005**, *94*, 350–357.

[3] "Adidas Brazuca." Wikipedia: The Free Encyclopedia. Wikimedia Foundation, Inc. (Accessed 17 Jun.. 2014).

[4] Hong, S.; Asai, T. Effect of panel shape of soccer ball on its flight characteristics *Scientific Reports* **2014**, *4*, 5068:1-7.

[5] Kroto, H. W.; Heath J. R.; O'Brien, S. C.; Curl, R. F.; Smalley, R. E. C_{60}: Buckminsterfullerene *Nature* **1985**, *318*, 162–163.

[6] Fowler, P. W.; Manolopoulos, D. E. *An Atlas of Fullerenes* Dover Publications, **2007**.

[7] Goldberg, M. A Class of Multi-Symmetric Polyhedra *Tohoku Math. J.* **1937**, *43*, 104–108.

[8] Caspar, D. L. D.; Klug, A. Physical Principles in the Construction of Regular Viruses *Cold Spring Harbor Symp. Quant. Biol.* **1962**, *27*,1–24.

[9] Manolopoulos, D. E.; Folwer, P. W. Molecular Graphs, Point Groups, and Fullerenes *J. Chem. Phys.* **1992**, *96*, 7603–7614.

[10] Fowler, P. W.; Cremona, J. E.; Steer, J. I. Systematics of Bonding in Non-Icosahedral Carbon Clusters *Theor. Chim. Acta.* **1988**, *73*, 1–26.

[11] Jendrol', S.; Kardoš, F. On Octahedral Fulleroids *Discrete Appl. Math.* **2007**, *155*, 2181–2186.

[12] Fowler, P. W.; Manolopoulos, D. E.; Redmond, D. B.; Ryan, R. P. Possible Symmetries of Fullerene Structures *Chem. Phys. Lett.* **1993**, *202*, 371–378.

[13] Fowler, P. W.; Rogers, K. M. Spiral Codes and Goldberg Representations of Icosahedral Fullerenes and Octahedral Analogues *J. Chem. Inf. Comput. Sci.* **2001**, *41*, 108–111.

[14] Tang, A.-C.; Huang, F.-Q. Electronic Structures of Octahedral Fullerenes *Chem. Phys. Lett.* **1996**, *263*, 733–741.

[15] Compernolle, S.; Ceulemans A. π Electronic Structure of Octahedral Trivalent Cages Consisting of Hexagons and Squares *Phys. Rev. B* **2005**, *71*, 205407.

[16] Compernolle, S.; Ceulemans, A. Frontier Orbitals of Trivalent Cages: (3,6) Cages and (4,6) Cages *J. Phys. Chem. A* **2005**, *109*, 2689–2697.

[17] Dunlap, B. I.; Taylor, R. Octahedral C_{48} and Uniform Strain *J. Phys. Chem.* **1994**, *98*, 11018–11019.

[18] Wu, H.-S.; Jiao, H.-J. What Is the Most Stable $B_{24}N_{24}$ Fullerene? *Chem. Phys. Lett.* **2004**, *386*, 369–372.

[19] Barone, V.; Koller, A.; Scuseria, G. E. Theoretical Nitrogen NMR Chemical Shifts in Octahedral Boron Nitride Cages *J. Phys. Chem. A* **2006**, *110*, 10844–10847.

[20] LaViolette, R. A.; Benson, M. T. Density Functional Calculations of Hypothetical Neutral Hollow Octahedral Molecules with a 48-Atom Framework: Hydrides and Oxides of Boron, Carbon, Nitrogen, Aluminum, and Silicon *J. Chem. Phys.* **2000**, *112*, 9269–9275.

[21] Rogers, K. M.; Fowler, P. W.; Seifert, G. Chemical Versus Steric Frustration in Boron Nitride Heterofullerene Polyhedra *Chem. Phys. Lett.* **2000**, *332*, 43–50.

[22] Zope, R. R.; Baruah, T.; Pederson, M. R.; Dunlap, B. I. Electronic Structure, Vibrational Stability, Infra-Red, and Raman Spectra of $B_{24}N_{24}$ Cages. *Chem. Phys. Lett.* **2004**, *393*,

300–304.

[23] Chuang, C.; Fan, Y.-C.; Jin, B.-Y. Generalized Classification Scheme of Toroidal and Helical Carbon Nanotubes *J. Chem. Inf. Model.* **2009**, *49*, 361–368.

[24] Chuang, C.; Fan, Y.-C.; Jin, B.-Y. Dual Space Approach to the Classification of Toroidal Carbon Nanotubes *J. Chem. Inf. Model.* **2009**, *49*, 1679–1686.

[25] Chuang, C.; Jin, B.-Y. Systematics of High-Genus Fullerenes *J. Chem. Inf. Model.* **2009**, *49*, 1664–1668.

[26] Chuang, C.; Fan, Y.-C.; Jin, B.-Y. Comments on structural types of toroidal carbon nanotubes, *J. Chin. Chem. Soc.* **2013**, *60*, 949–954.

[27] Chuang, C.; Fan, Y.-C.; Jin, B.-Y. Systematics of Toroidal, Helically-Coiled Carbon Nanotubes, High-Genus Fullerenes, and Other Exotic Graphitic Materials *Procedia Eng.* **2011**, 14, 2373–2385.

[28] Chuang, C; Jin, B.-Y. Classification of Hypothetical Doubly and Triply Periodic Porous Graphitic Structures by Tilings of Neck-Like Units *J. Math. Chem.* **2010**, *47*, 1077–1084.

[29] Fujita, S. Symmetry and Combinatorial Enumeration in Chemistry Springer-Verlag, **1991**.

[30] Tománek, D. *Guide Through the Nanocarbon Jungle: Buckyballs, Nanotubes, Graphene and Beyond* IOP Concise Physics series, Morgan & Claypool Publishers, **2014**.

[31] Delp, K.; Thurston, B. Playing With Surfaces: Spheres, Monkey Pants, and Zippergons *Proceedings of Bridges 2011: Mathematics, Music, Art, Architecture, Culture* **2011**, 1–8.

[32] Šiber, A. Shapes and energies of giant icosahedral fullerenes *Euro. Phys. J. B* **2006**, *53*, 395-400.

[33] Yong, E. U.; Nelson, D. R.; Mahadevan, L. Elastic Platonic Shells *Phys. Rev. L.* **2013**, *111*, 177801:1-5.